

タイトル	Properties of computer-simulated fractal speckles
著者	Uozumi, Jun
引用	工学研究：北海学園大学大学院工学研究科紀要(21): 3-17
発行日	2021-12-24

# Properties of computer-simulated fractal speckles

Jun Uozumi\*

## Abstract

Fractal speckles are simulated in a computer by assuming that a uniformly distributed random phase screen is illuminated by coherent light with an intensity profile of a power function. The results are discussed in comparison with the previous theoretical and experimental papers by the author's group. For the power  $-D$  of the power function, a wider range of  $0 < D \leq 3$  is examined than that of  $1 < D < 3$  discussed in the theory. From the simulated speckle intensities, probability density function (PDF), speckle contrast, and spatial correlation function are derived. The fractality of speckles predicted theoretically in the range of  $1 < D < 2$  is confirmed by the simulation on the basis of the result that the intensity correlation function obeys a power function with the power of  $2(D - 2)$ . It is revealed from the PDF and contrast that the speckle in this range is fully developed and obeys the zero-mean circular complex Gaussian statistics. Even in this range, however, the speckle shows a slight deviation from this statistics as  $D$  approaches to 2, and when  $D$  exceeds 2, the speckles no longer obey this statistics. It is also revealed that the fractality of speckles is extended to the missing region of  $0 < D < 1$  in the theoretical analysis, though adequate care is needed in the interpretation of the fractal dimension in this region.

**Key Words** : fractal speckle, fractal dimension, computer simulation, power-law illumination, intensity correlation

## 1. Introduction

Speckles can be regarded as random markers distributed over the two- or three-dimensional space, which make it possible to detect various mechanical information of an object generating the speckles, or lying or moving in the space.<sup>1,2)</sup> Therefore, the spatial extent of the marker, namely the speckle size, is a critical factor affecting the specifications, such as sensitivity, detection range and dynamic range, of the detecting method using speckles.

The speckle size is given by the intensity correlation function of speckles, which is typically determined by the Fourier transform of an intensity profile of light incident on the scattering object as far as the speckles are observed in the

Fraunhofer diffraction region of the scattering object and obey the complex Gaussian statistics. Therefore, elaborating the intensity profile incident on the diffuser is the fundamental principle of controlling the intensity correlation of speckles.

To generate speckles with very long spatial correlation, Uno et al.<sup>3)</sup> proposed theoretically a method for generating fractal speckles, which have intensity correlation obeying a power function. This type of fractal speckles was then confirmed experimentally.<sup>4)</sup> After that, various properties of the fractal speckles have been revealed theoretically and experimentally.<sup>5-12)</sup>

In addition, computer simulation studies have also been carried out by the present author to complement theoretical analysis, and the results have been shown in a summarized form in several

---

\* Graduate School of Engineering (Electronics, Information and Life Science Eng.), Hokkai-Gakuen University

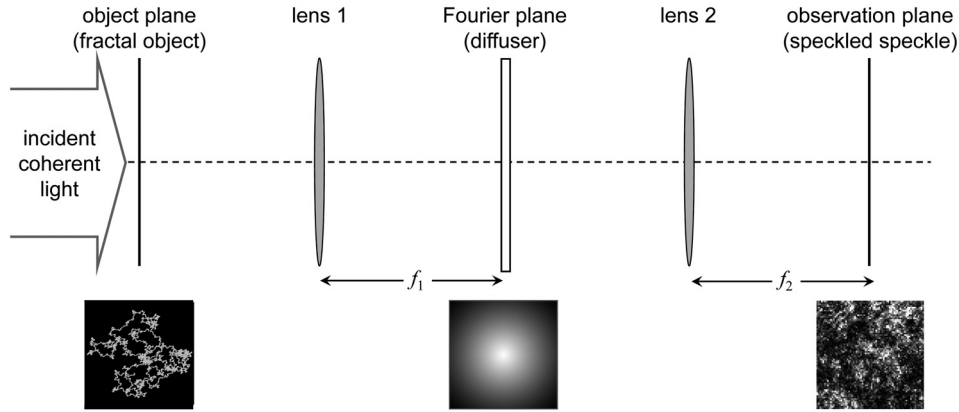


Fig. 1 Optical system for generating fractal speckles by a double scattering process.

reports as conference proceedings.<sup>13-15)</sup> However, detailed description of the simulation study has not been given so far.

The purpose of this paper is to describe the procedures of the computer simulation of fractal speckles in detail with results of higher precision than given ever, and to have discussions, in particular, in comparison with the previous theoretical and experimental results.

## 2. Theoretical background

In the theoretical analysis carried out by Uno et al.,<sup>3)</sup> a doubly scattered speckle, or speckled speckle, was assumed for the generation of fractal speckles. With reference to Fig.1, incident coherent light is first scattered by a random fractal object with fractal dimension  $D$  and produces in its far field or in its Fourier transform plane a speckle pattern, a kind of diffractal, as coined by Berry<sup>16)</sup>. This diffractal speckle has an average intensity distribution expressed by

$$I(\mathbf{q}) \propto q^{-D}, \quad (1)$$

where  $\mathbf{q}$  is a position vector of this observation plane and  $q$  is its magnitude, i.e. the distance from the optical axis. Equation (1) is a well-known relation for the small-angle scattering from a mass fractal object of dimension  $D$ .<sup>17-19)</sup>

This speckle field is subsequently scattered by an ordinary diffuser such as a ground glass plate placed in the plane, and a doubly scattered field is generated in the far field of the ordinary

diffuser. Uno et al. showed that the correlation function  $\mu(r)$  of the intensity variations of this speckle field is given by

$$\mu(r) = \frac{\langle I(r')I(r'+r) \rangle - \langle I(r') \rangle \langle I(r'+r) \rangle}{\langle I(r') \rangle \langle I(r'+r) \rangle}$$

$$\infty \begin{cases} r^{2(D-2)} & ; 1 < D < 2 \\ (\log r)^2 & ; D = 2 \\ 1 & ; 2 < D < 3 \end{cases} . \quad (2)$$

It is known in the theory of fractals that a non-negative physical quantity  $M$  is fractal with fractal dimension  $D$  if  $M$  has an autocorrelation function of the form of a power function

$$C(\chi) = \langle M(\mathbf{x})M(\mathbf{x}+\chi) \rangle \propto \chi^{-\alpha} \quad (3)$$

with the power  $\alpha$  equal to  $d-D$  where  $d$  is the Euclidean dimension of the observation space. Therefore, from eq. (2), this type of doubly scattered speckles under the condition of  $1 < D < 2$  can be considered to be fractal, and the fractal dimension  $D_s$  of the speckle is given by<sup>18,19)</sup>

$$D_s = 2D - 2. \quad (4)$$

This theoretical prediction was verified by an experiment based on the double scattering by a random fractal object and a ground glass plate as an ordinary diffuser.<sup>4)</sup>

It is noted that most important factor for producing fractal speckle is that the second ordinary diffuser is illuminated by coherent light having the intensity profile of eq. (1) as shown in Fig. 2. Therefore, the role of the first scattering by the random fractal object is to generate this

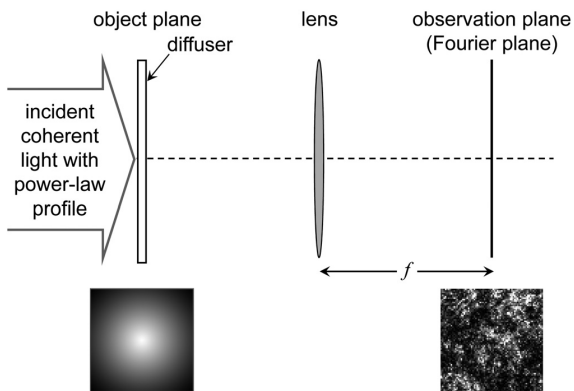


Fig. 2 Optical system for generating fractal speckles by a simple scattering process.

power-law profile for illuminating the diffuser. This fact was clearly verified by Funamizu and Uozumi,<sup>5)</sup> who produced fractal speckles by generating coherent illumination profile in the form of eq. (1) by means of a spatial light modulator.

Statistical properties of fractal speckles have been investigated by the author's group; three-dimensional correlation property,<sup>10)</sup> generation and properties in an image plane<sup>9)</sup> and a Fresnel diffraction region,<sup>11)</sup> multifractality,<sup>7)</sup> derivatives of intensity and phase,<sup>12)</sup> and so on.

It is also noted that the experiments made so far were limited to the case of  $1 < D < 2$ . This is because there are some difficulties in carrying out experiments for  $D \geq 2$ . Since ordinary fractal apertures embedded in a plane have a fractal dimension  $D$  less than the Euclidean dimension  $d=2$  inevitably. This limitation may be bypassed by exploiting surface fractals.<sup>20,21)</sup> That is, an aperture with its marginal boundary being fractal line with a surface fractal dimension  $D_b$  produces, on diffraction, the intensity distribution proportional to  $q^{-(2d-D_b)}$ , which amounts to  $q^{-D}$  with  $2 < D \leq 3$  for  $2 > D_b \geq 1$ . However, power functions with such a strong decay require extremely low noise conditions for reliable experiments.

It is also noted that eq. (2) states nothing about the case of  $D \leq 1$ . Scattering experiment in this regime involves another difficulty. That is, objects with small  $D$  have extremely small transmittance and, therefore, yield extremely low intensity distribution in the Fourier plane in Fig. 1.

Because of these difficulties in experiments for the ranges of  $D$  outside of  $1 < D < 2$ , computer simulations were employed for investigating the correlation properties of speckles produced in the entire range of  $0 \leq D \leq 3$ . The present paper describes the same procedure of the computer simulations performed in the past studies,<sup>13-15)</sup> but in more detail and with higher precision.

### 3. Simulation procedure

With reference to Fig. 2, a square matrix of a size  $N \times N$  is generated from uniform and uncorrelated random numbers in the range of  $(-\pi, \pi)$  to model a random phase distribution  $\phi(\mathbf{q})$  of a diffuser placed in the object plane, where  $N=2^{13}=8192$  is used in the present simulation, while it was  $N=2^{10}=1024$  in the previous one.<sup>13-15)</sup>

A complex amplitude for illuminating the diffuser is given by a matrix expressed by, instead of the square root of eq. (1), the function of

$$A(\mathbf{q}) = \left[ 1 + \left( \frac{q}{R} \right)^2 \right]^{-\frac{D}{4}}, \quad (5)$$

which is a typical approximation to a power function for avoiding the singularity at the origin.<sup>21)</sup> In eq. (5),  $R$  stands for the parameter controlling a deviation of this approximation from the precise power function around the origin. Figure 3 shows  $A(\mathbf{q})$  of eq. (5) in a logarithmic graph for three different values of  $R$  and for  $D=1$ .

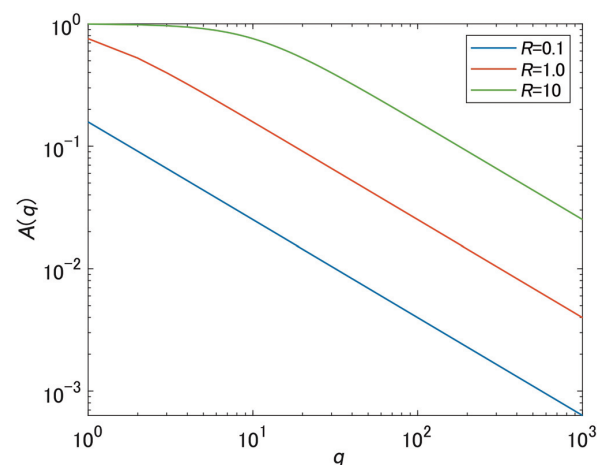


Fig. 3 Dependence of the incident complex amplitude  $A(\mathbf{q})$  on the parameter  $R$ .



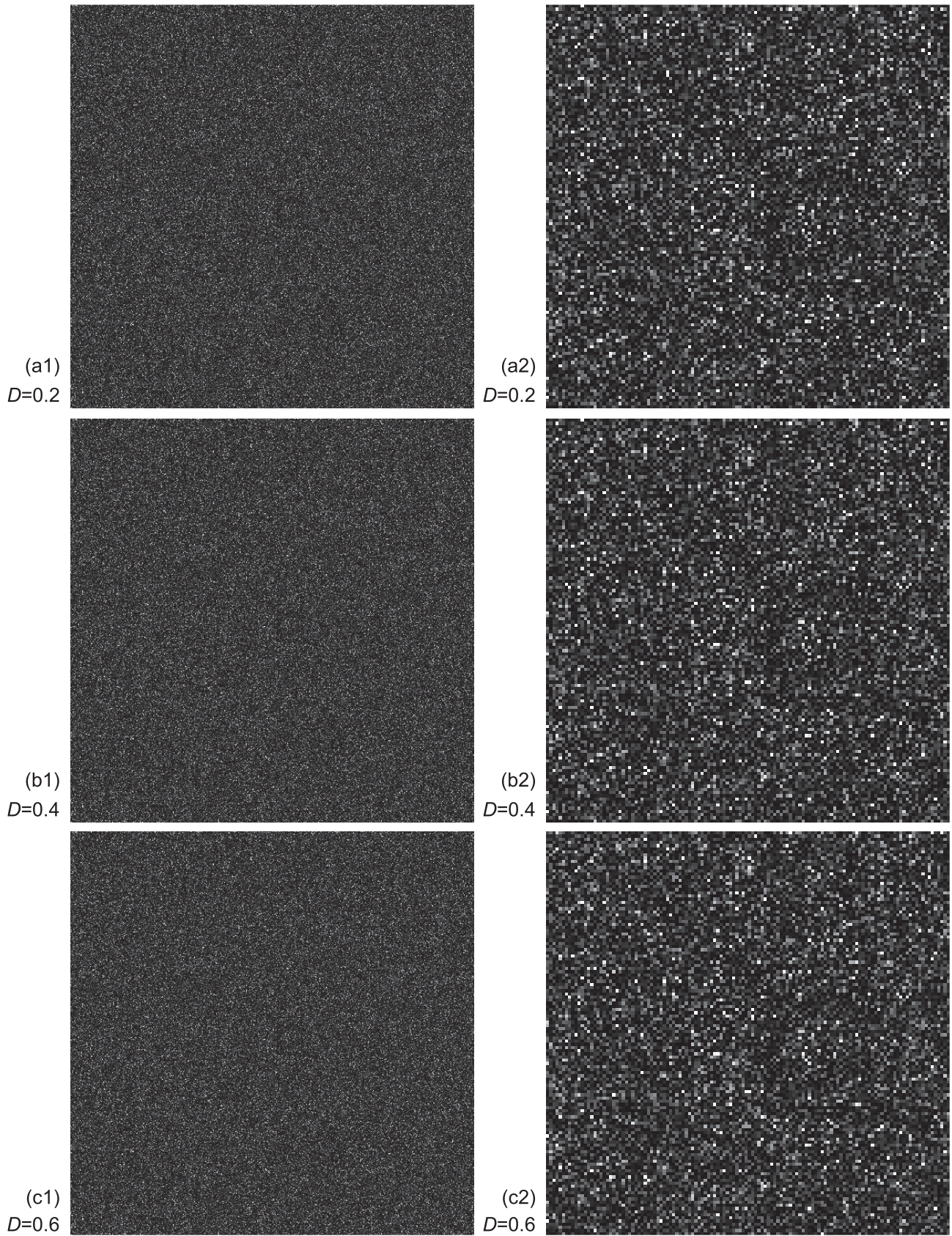


Fig. 4 Speckle patterns for  $0.2 \leq D \leq 1.0$ . Patterns of (a1)–(e1) are of  $1024 \times 1024$  pixels, while those of (a2)–(e2) are magnified central area of  $128 \times 128$  pixels of them.



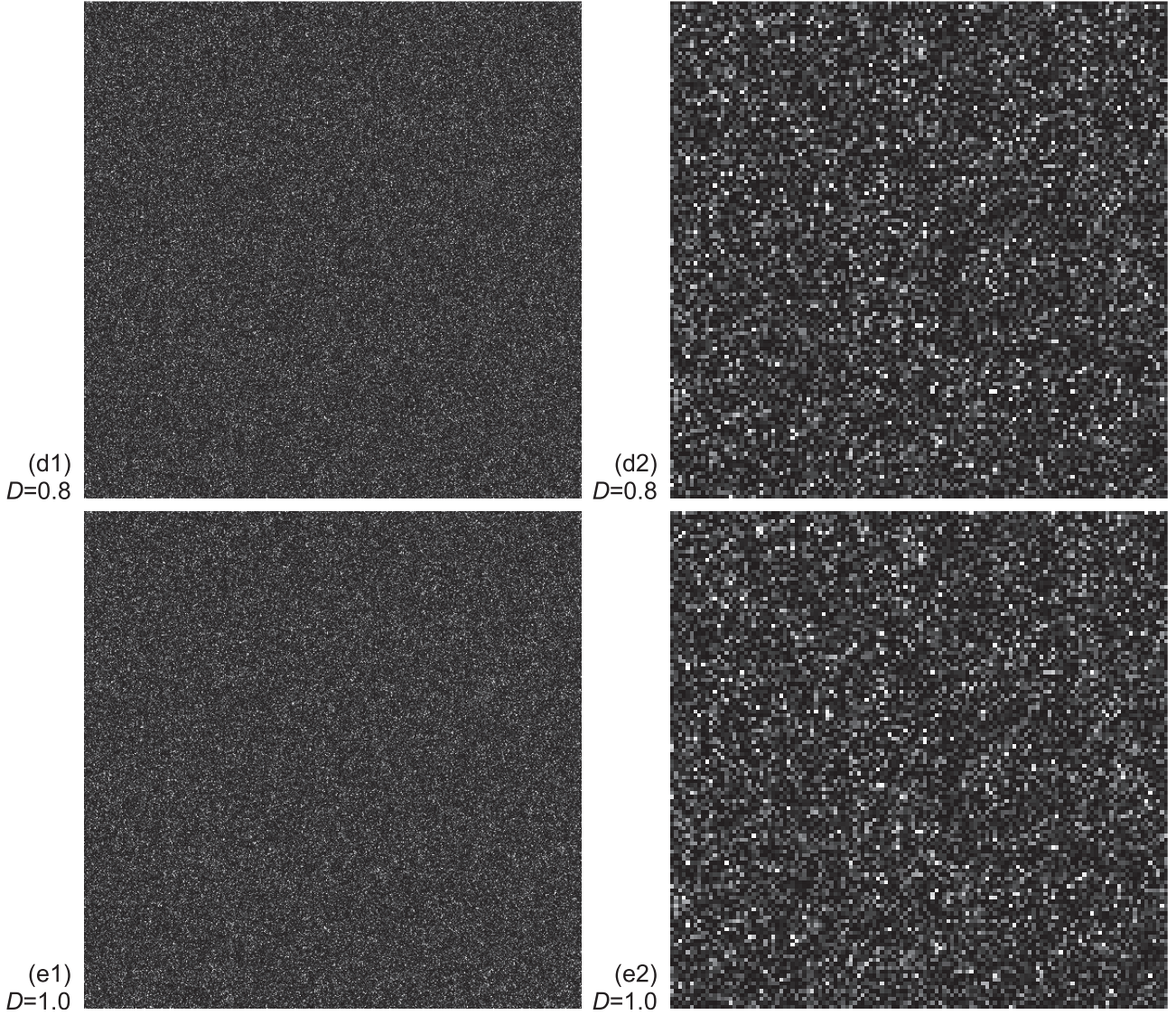


Fig. 4 (continued)

4. It is seen from this figure that  $R$  corresponds nearly to the center of the crossover region from the constant to the power-function behaviors as expected from eq. (5). We adopted  $R=0.1$  since it gives almost perfect power function except at the origin, where  $A(0)=1$ .

The complex amplitude distribution just behind the diffuser is calculated from two matrices of  $\exp[i\phi(\mathbf{q})]$  and  $A(\mathbf{q})$ , and hence, the intensity distribution in the observation plane is obtained by

$$I(\mathbf{r}) = |\text{FFT2}\{A(\mathbf{q})\exp[i\phi(\mathbf{q})]\}|^2, \quad (6)$$

where  $\text{FFT2}\{\}$  stands for the two-dimensional fast Fourier transform operation.

From this intensity distribution, the probability density function  $p(I)$  and the speckle contrast defined by

$$C = \frac{\sigma_I}{\langle I \rangle} \quad (7)$$

are directly derived, in which  $\langle I \rangle$  and  $\sigma_I$  are the average and standard deviation of the intensity. The intensity correlation function is also calculated by the first equality in eq. (2). For Monte Carlo simulations based on random numbers, reduction of statistical fluctuations in the results is quite important. In the present simulation, the statistical noise in the intensity correlation function is reduced in two ways. First, an ensemble average of the two-dimensional correla-



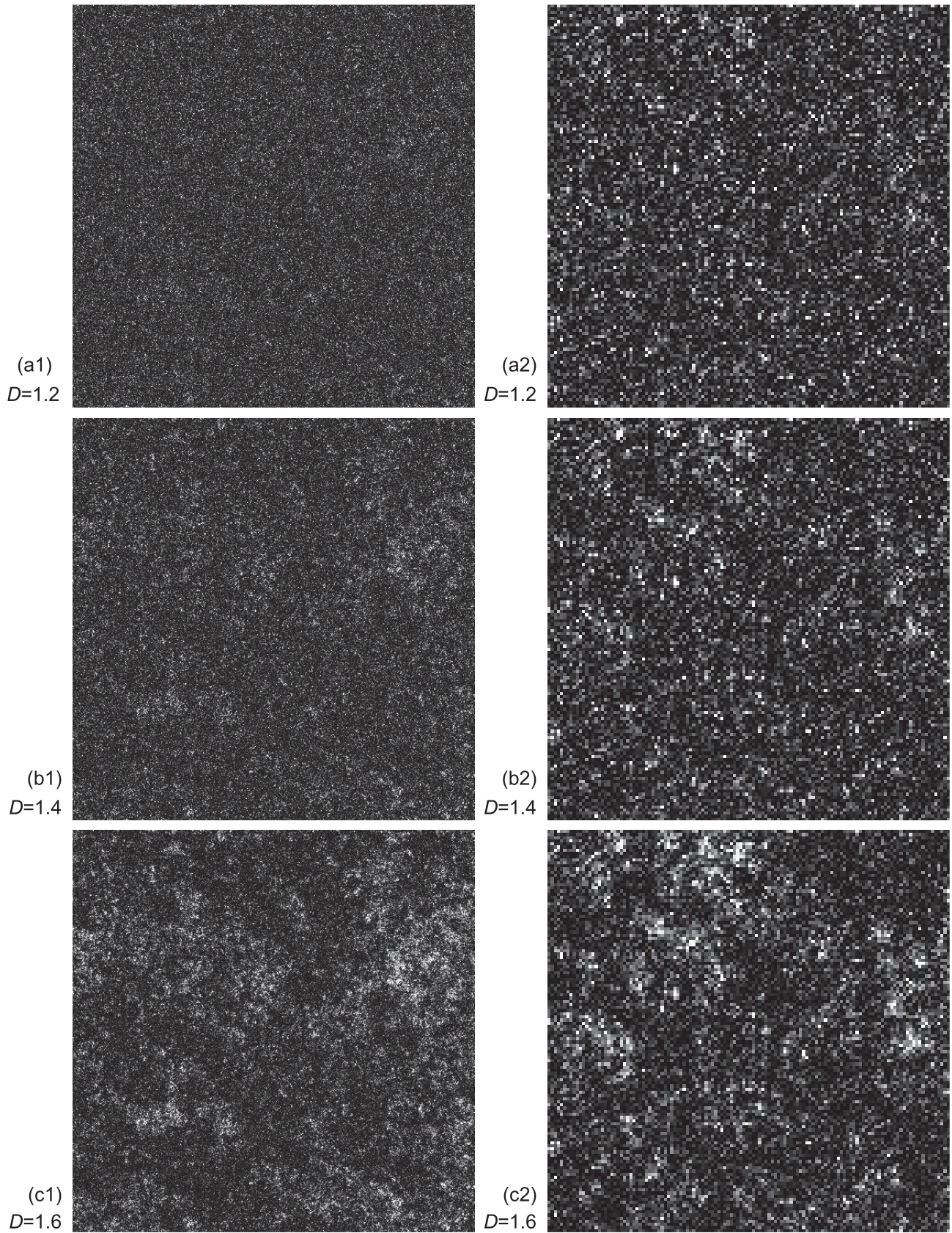


Fig. 5 Speckle patterns for  $1.2 \leq D \leq 2.0$ . Patterns of (a1)–(e1) are of  $1024 \times 1024$  pixels, while those of (a2)–(e2) are magnified central area of  $128 \times 128$  pixels of them.



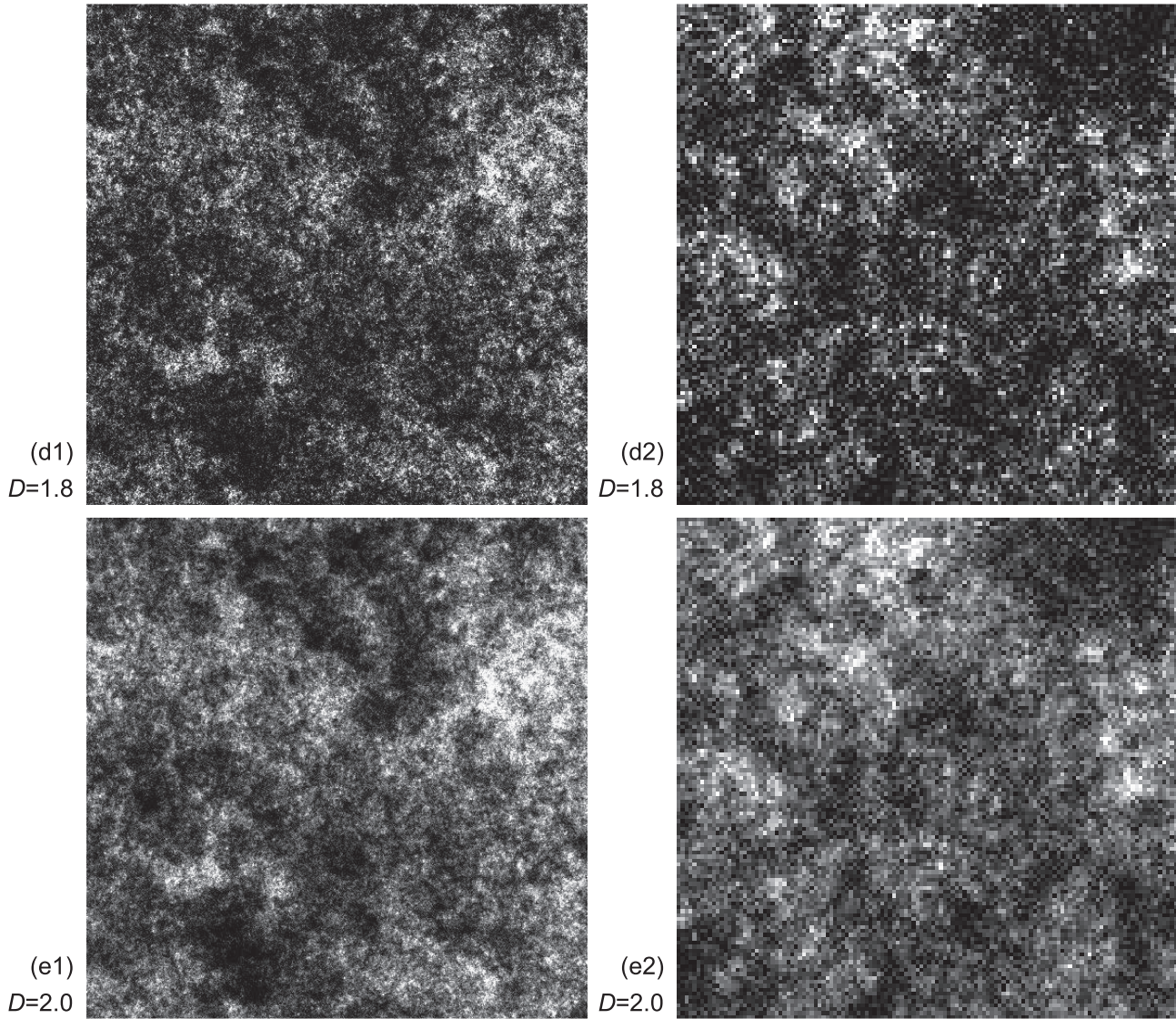


Fig. 5 (continued)

tion function is calculated from a large number of speckle patterns produced by statistically independent random number matrices, which correspond physically to statistically independent rough surfaces or phase screens. Second, by virtue of the isotropy of the phenomenon, an angular average of the ensemble averaged correlation function is calculated by

$$C_I(r) = \frac{1}{2\pi} \int_0^{2\pi} C_I(r, \theta) d\theta. \quad (8)$$

This angular average is effective and employed also in processing experimental data.<sup>4)</sup> Simulations and the related calculations are all performed with MATLAB.

## 4. Results and discussions

### 4.1 Intensity distributions

Some examples of speckle patterns generated by the simulation are shown in Figs. 4-6 for every 0.2 value in the range of  $0.2 \leq D \leq 3.0$ . In these figures, images of (a1)-(e1) show speckles in an area of  $1024 \times 1024$  pixels, for which speckles are displayed in such a way that  $I=0$  and  $I \geq \langle I \rangle + 4C$  correspond to black and white, respectively, while those of (a2)-(e2) are their magnified central portions of  $128 \times 128$  pixels, in which each pixel is barely resolved. Let us use (a) to denote both of (a1) and (a2), and the similar notations for (b)-(e),



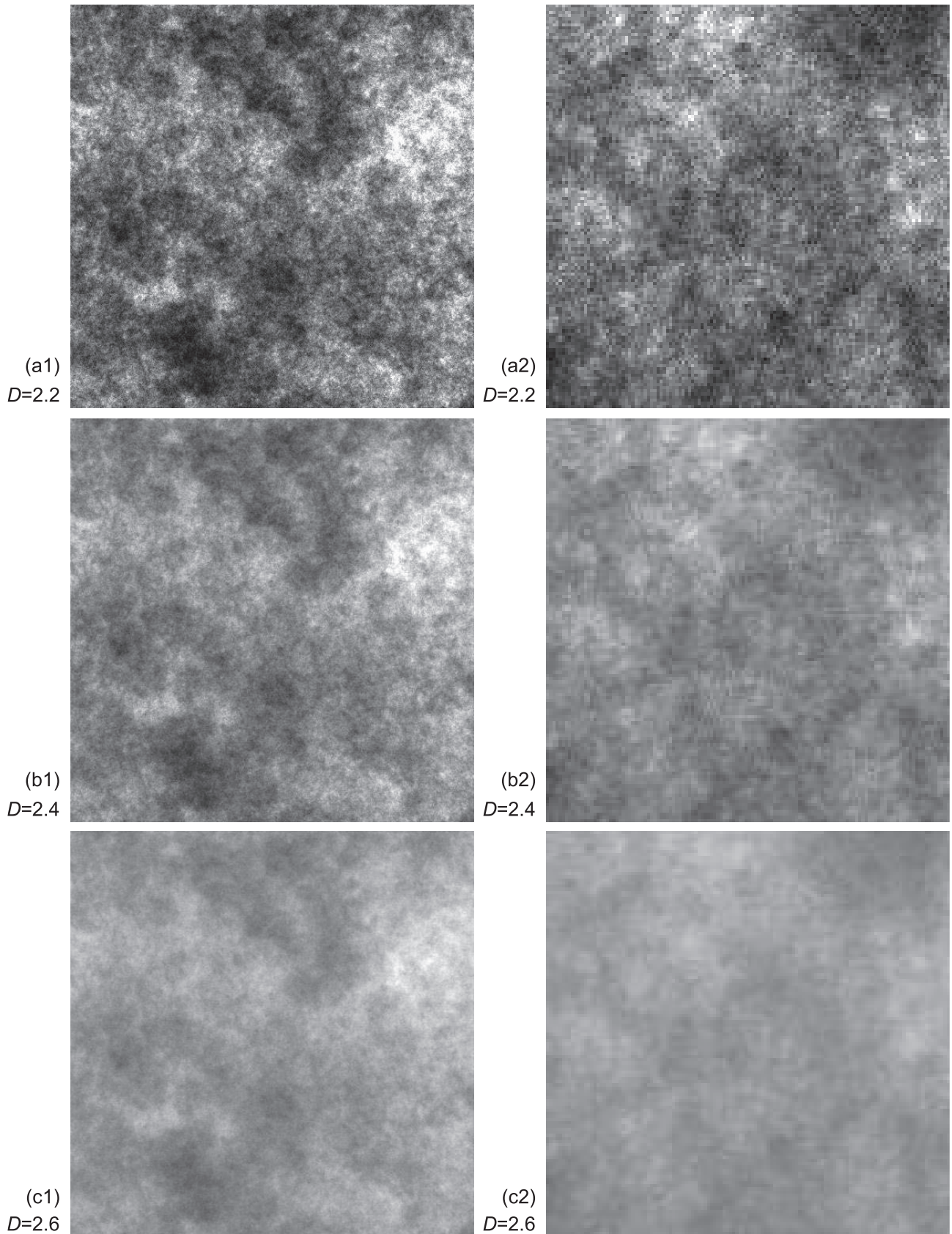


Fig. 6 Speckle patterns for  $2.2 \leq D \leq 3.0$ . Patterns of (a1)–(e1) are of  $1024 \times 1024$  pixels, while those of (a2)–(e2) are magnified central area of  $128 \times 128$  pixels of them.

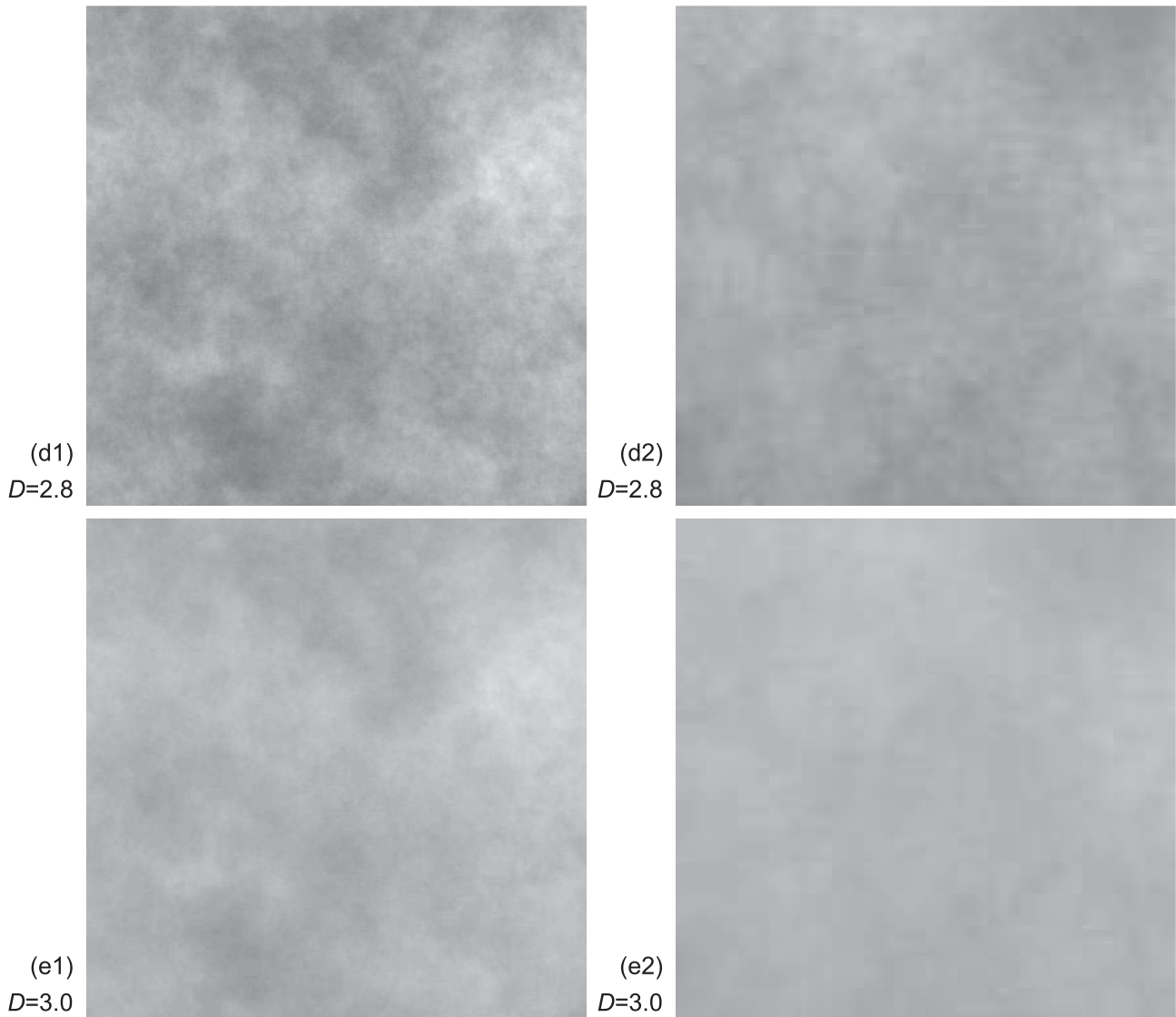


Fig. 6 (continued)

too.

Figures 4(a)–(e) show the case of  $0.2 \leq D \leq 1.0$ , which is not covered by eq. (2). From the figures of (a1)–(e1), it is seen that speckle grains are very small and seem to distribute almost independently from each other. However, close observation of the magnified portions in (a2)–(e2) reveals that some speckle grains grow and some diminish gradually and slightly with an increase in  $D$  even in this regime. It seems difficult, however, to judge from these patterns whether these intensity distributions have fractal property.

Figures 5(a)–(e) correspond to the range of  $1.2 \leq D \leq 2.0$ , which is the regime where the fractality is predicted by eq. (2), except the case of  $D=2.0$ ,

and confirmed experimentally.<sup>4)</sup> The intensity distributions in this region correspond well to the experimental patterns (Fig. 4 in ref.<sup>4)</sup>, and hence the simulation visually confirms again the absence of definite speckle size, statistically self-similar appearances, and monotonous development of intensity clustering with an increase in  $D$ . In case of  $D=2.0$  shown in Fig. 5(e), however, fine details of intensity variations in the speckle pattern begin to weaken. This fact implies the deviation from fractal behavior predicted in eq. (2).

When the exponent  $D$  increases further and enter the regime of  $D > 2.0$ , the intensity distributions come to show different appearances from those in the region of  $1.0 < D < 2.0$ . As is seen from



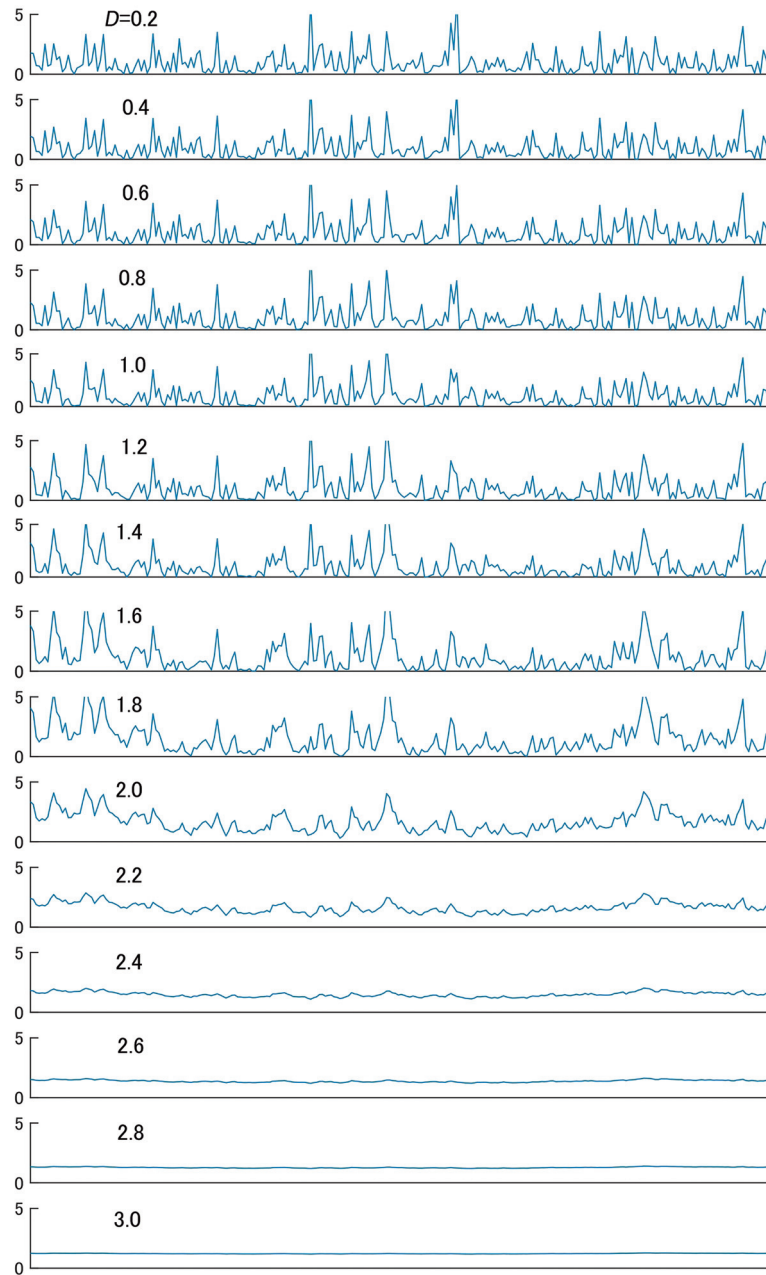
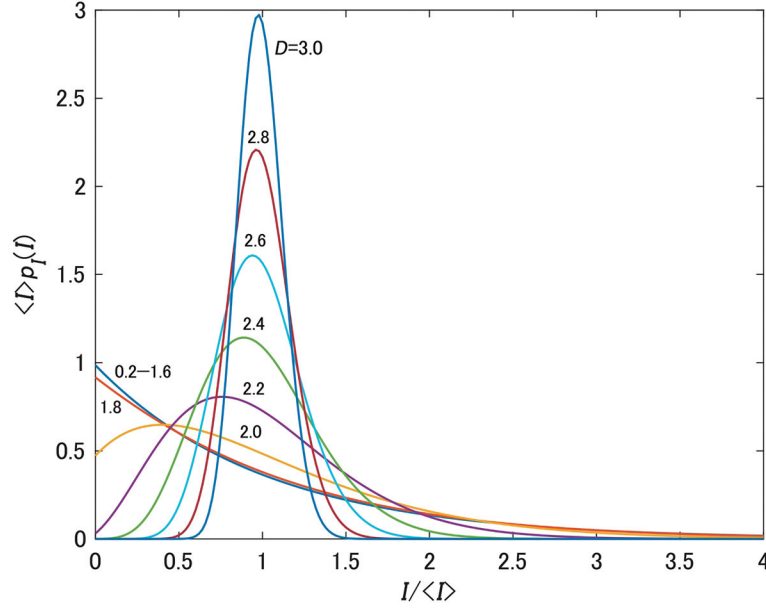


Fig. 7 Intensity distributions along horizontal central lines of Figs. 4(a1)–(e1), 5(a1)–(e1) and 6(a1)–(e1).

Fig. 6(a)–(e), the patterns seem to loose granular appearance gradually and to gain rather smooth structures instead. Such a trend can be explained qualitatively as follows. Since the observation plane is located in the Fourier transform plane of the diffuser and since the diffuser behaves as a white noise generator, the illuminating intensity distribution can be regarded as a power spectrum of the complex amplitude in the observation plane. Therefore, the power-law illumination with very large value of  $D$  corresponds to a strong

enhancement of the DC and lower spatial frequency components and considerable suppression of higher frequency components in the scattering patterns.

Intensity distributions along the horizontal central lines of Figs. 4(a1)–(e1), 5(a1)–(e1) and 6(a1)–(e1) are shown in Fig. 7 for the length of 256 pixels. In this figure, the intensities are normalized by its average  $\langle I \rangle$ . Important features in appearance of speckles explained above, namely very slight and gradual growth and diminution of intensity peaks

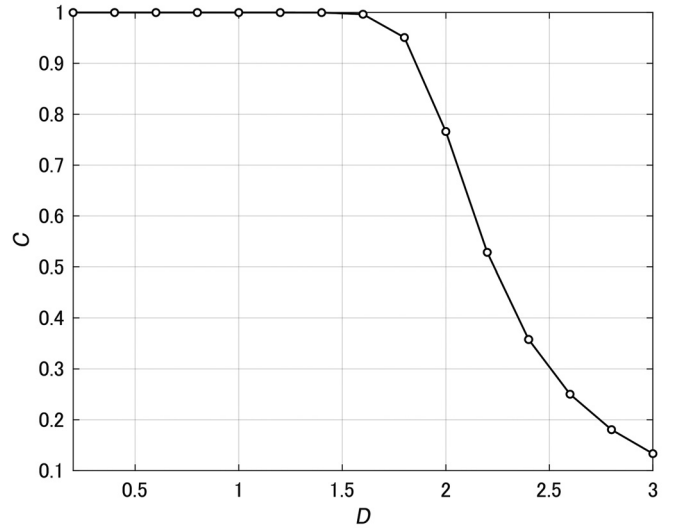

 Fig. 8 Dependence of the PDF of intensity on  $D$ .

from  $D=0.2$  to  $D=1.0$ , subsequent clear growth of speckle clustering up to  $D=1.8$ , and then turning to gradual loss of fine structures and peaks beyond  $D=2.0$ , can be verified in this figure.

#### 4.2 Probability density function and Contrast

The PDF,  $p_i(I)$ , of the speckle intensity is calculated as a normalized histogram and the result is shown in Fig. 8. In the calculation of PDF in Fig. 8, the data were averaged over statistically independent 2000 diffusers. It is seen from this figure that the speckle intensity practically obeys the negative exponential density for  $0.2 \leq D \leq 1.6$ , shows a slight deviation from that for  $D=1.8$ , and gradually approaches to Gaussian-like density with a further increase in  $D$ . This implies that the speckle is fully developed and obeys the zero-mean circular complex Gaussian statistics for  $0.2 \leq D \leq 1.6$ .<sup>22, 23)</sup> Then the speckle begins to deviate from it as  $D$  approaches to and exceeds 2.0. This behavior of PDF agrees with the experimental result shown in ref.<sup>4)</sup>, in which it was shown that the experimental PDF is of the negative exponential for  $D=1.2, 1.5$  and 1.8.

Speckle contrast  $C$  is also calculated by eq. (7) from the simulated speckle patterns generated from 2000 diffusers, and the result is shown in Fig.


 Fig. 9 Dependence of the speckle contrast on  $D$ .

9. It is seen from this figure that the contrast is practically unity for  $D \leq 1.6$ , with a very slight decrease for  $D=1.6$ . Then it begins to decrease around  $D=1.8$ , and rapid decrease is observed with a further increase in  $D$  in the region of  $D \geq 2.0$ . From this behavior of the contrast, together with the PDF of the intensity shown in Fig. 8, we can conclude that the speckle in the range of  $0.2 \leq D \leq 1.6$  is fully developed. This is an interesting result because it is difficult to estimate an effective number of independent scattering elements included in the illuminating spot in the case of the



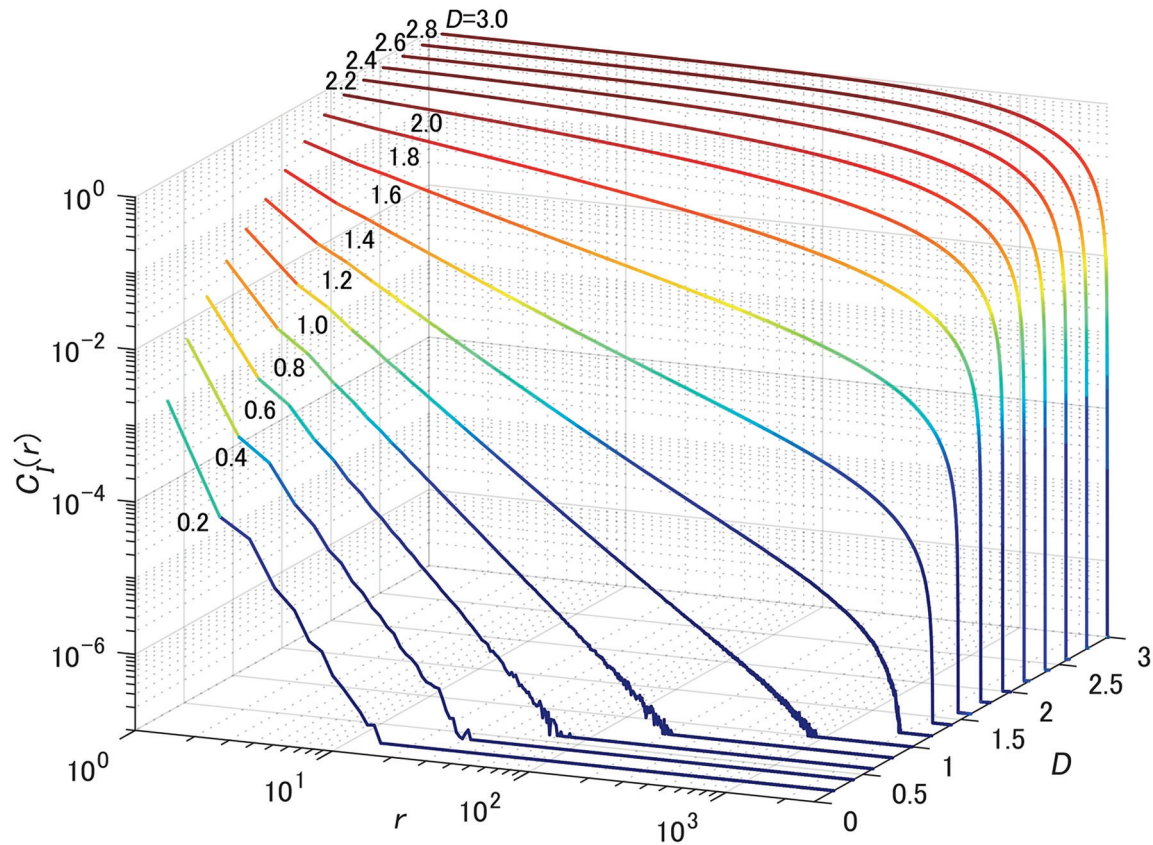


Fig. 10 Dependence of the intensity correlation function on the exponent  $D$ .

power-law illumination, which has no definite spot size as shown in Fig. 2 and hence we have no evidence to justify the application of the central limit theorem in the formation of the fractal speckles.

#### 4.3 Intensity correlation and fractal dimension

Intensity correlation functions are calculated from the intensity distributions shown in Figs. 4–6 together with other similar patterns and are shown in Fig. 10 as a three-dimensional plot. The number of statistically independent diffusers used in calculating  $C_I(r)$  in Fig. 10 was 200,000 for  $D=0.2$ , 100,000 for  $0.4 \leq D \leq 1.0$ , 20,000 for  $D=1.2$  and  $1.4$ , and 2,000 for  $1.6 \leq D \leq 3.0$ . Due to these large numbers of diffusers, the correlation function is derived with much higher precision than given in the previous reports.<sup>13–15</sup> In Fig. 10, one horizontal axis,  $r$ , and the vertical axis,  $C_I(r)$ , are plotted on a logarithmic scale, while the other horizontal axis,

$D$ , linearly. It follows that a linear behavior in planes parallel to the  $C_I(r) - r$  plane implies a power function. It is clearly seen from this figure that  $C_I(r)$  is regarded as power functions in the regime of  $1 < D < 2$  for the range of  $r \lesssim 10^2$ , and that the slope of the line becomes steeper as  $D$  decreases. This agrees with the theoretical prediction of eq. (2) and experimental data (Fig. 8 in ref.<sup>4</sup>). We can also confirm that the correlation function is practically constant for  $D > 2$ , and that  $D=2$  is the critical point between the power-law behavior and constant one, which is predicted also in eq. (2). Of course, this nearly constant behavior for  $D > 2$  corresponds to the rather smooth appearance of the patterns in Fig. 6 and gradually flattening intensity distribution for  $D > 2$  in Fig. 7.

On the other hand, it is interesting to note that the power-law behavior in the regime of  $1 < D < 2$  seems to be extrapolated to that of  $D \leq 1$ . Thus, the range of  $D$  that produces fractal correlation property is extended toward the lower  $D$  than predicted by eq. (2). This means that the

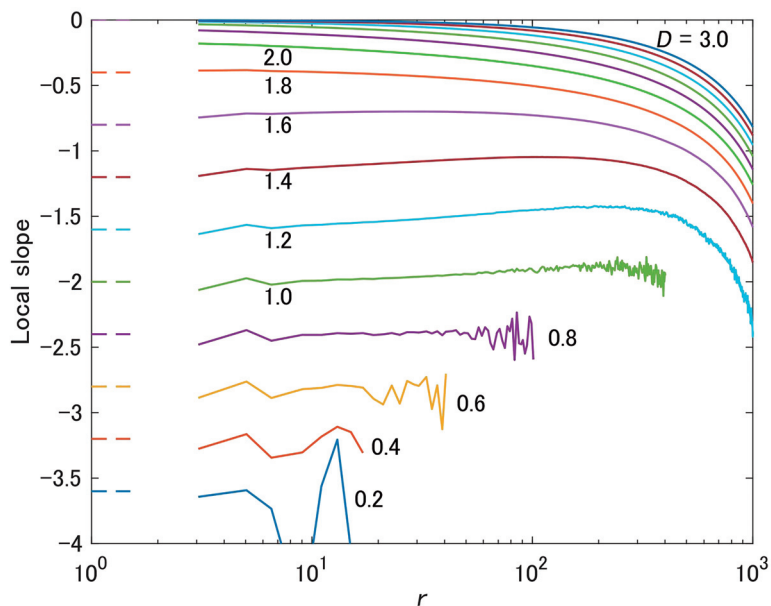


Fig. 11 Local slope of  $C(r)$  in the logarithmical plot.

degree of spatial correlation of the fractal intensity distributions can be controlled in a wider range than considered so far.

For quantitative examination of the apparently linear behavior of  $C(r)$  in Fig. 10, the local slope of each curve is calculated and shown in Fig. 11. In this figure, the slope predicted by eq. (2) is also shown on the left with short broken lines, each with the same color as the corresponding local slope curve, with the predicted values extrapolated to  $D < 1.0$ . It is seen in this figure that each local slope is nearly constant in the range of  $r \lesssim 10^2$ , though still remaining statistical fluctuations become stronger as  $D$  decreases. The local slopes show fairly good accordance with the theoretical slope for  $D \leq 1.8$  including also the extrapolated regime of  $D \leq 1.0$ , though slight variations are also observed in each curve.

As discussed in sec. 2, the fractal dimension  $D_s$  of the speckle patterns in the case of  $1 < D < 2$  is given by eq. (4), which covers the range of  $0 < D_s < 2$ . However, extrapolation of this relation to  $D \leq 1$  gives rise to negative values of  $-1 \leq D_s \leq 0$ . This is not acceptable and is to be interpreted to be  $D_s = 0$  in this region. This peculiarity is explained as follows. The discussion made so far is based on the two-dimensional observation plane. However, the speckling phenomenon under current discussion

is not restricted in the two-dimensional observation plane but is known to extend in the three-dimensional space, and therefore the fractal structure is also extended in the three-dimensional space.<sup>10)</sup> If this three-dimensional fractality is isotropic, the fractal dimension of the three-dimensional distribution of speckle would be  $D_s + 1$ . Hence, the apparently negative dimension in the two-dimensional plane is non-negative in the three-dimensional space. It is noted, however, that the fractality in the three-dimensional space is known to be anisotropic.<sup>10,11)</sup> Therefore, the discussion concerning the fractal dimension of speckles in the three-dimensional space would be more complicated, and worth further discussions.<sup>24)</sup>

## 5. Conclusion

Generation of speckles was simulated in a computer by assuming that a uniformly distributed random phase screen is illuminated by coherent light with an intensity profile of a power function. For the power  $-D$  of the power function, a wider range of  $0 < D \leq 3$  was examined than that of  $1 < D < 3$ , covered in the previous theoretical treatment.

The generated speckles show a very slight and gradual growth and diminution of intensity



peaks with an increase in  $D$  from  $D=0.2$  to  $D=1.0$ , and subsequently clear growth of speckle clustering is observed up to  $D=1.8$ , and then they turn to gradual loss of fine structures and peaks beyond  $D=2.0$ .

From the simulated speckle intensities, probability density function (PDF), speckle contrast, and spatial correlation function were derived. The fractality of speckles predicted theoretically in the range of  $1 < D < 2$  was confirmed by the simulation, on the basis of the result that the intensity correlation function obeys a power function with the power nearly equal to the theoretical values of  $2(D-2)$ .

It is revealed from the PDF and contrast that the speckle in this range is fully developed and obeys the zero-mean circular complex Gaussian statistics. Even in this range, however, the speckle shows a slight deviation from this statistics as  $D$  approaches to 2, and when  $D$  exceeds 2, the speckles no longer obey this statistics.

It was also revealed that the fractality of speckles is extended to the missing region of  $0 < D < 1$ , in the theoretical analysis. This is an interesting result though adequate care is needed in the interpretation of the fractal dimension in this region.

## References

- 1) R. K. Erf, ed.: *Speckle Metrology*, Academic, New York, 1978.
- 2) R. S. Sirohi, ed.: *Selected Papers on Speckle Metrology*, SPIE Milestone Series Vol. MS 35, SPIE, Washington, 1991.
- 3) K. Uno et al.: Correlation properties of speckles produced by diffractal-illuminated diffusers, *Opt. Commun.*, **124**(1, 2), pp. 16-22 (1996).
- 4) J. Uozumi et al.: Fractal speckles, *Opt. Commun.*, **156**(4-6), pp. 350-358 (1998).
- 5) H. Funamizu and J. Uozumi: Generation of fractal speckles by means of a spatial light modulator, *Opt. Express*, **15**(12), pp. 7415-7422 (2007).
- 6) J. Uozumi: Phase singularity distribution of fractal speckles, *Proc. 2<sup>nd</sup> Internat. Conf. Optics and Laser Applications (ICOLA'07)*, Yogyakarta, Indonesia, pp. 16-20 (2007).
- 7) H. Funamizu and J. Uozumi: Multifractal analysis of speckle intensities produced by power-law illumination of diffusers, *J. Modern Opt.*, **54**(10-12), pp. 1511-1528 (2007).
- 8) H. Funamizu and J. Uozumi: Scaling reduction of the contrast of fractal speckles detected with a finite aperture, *Opt. Commun.*, **281**(4), pp. 543-549 (2008).
- 9) E. Miyasaka and J. Uozumi: Generation of fractal speckles in image plane and their application to the measurement of displacement, *Engineering Research (Bull. Grad. Sch. Eng., Hokkai-Gakuen Univ.)*, No. 12, pp. 13-23 (2012).
- 10) M. Ibrahim and J. Uozumi: Three-dimensional correlation properties of speckles produced by diffractal-illuminated diffusers, *Asian J. Phys.*, **27**(9-12), pp. 457-466 (2018).
- 11) K. Tsujino and J. Uozumi: Correlation properties of fractal speckles in the Fresnel diffraction region, *Asian J. Phys.*, **27**(9-12), pp. 515-528 (2018).
- 12) H. Funamizu and J. Uozumi: Statistics of derivatives of intensity and phase of fractal speckles, *Asian J. Phys.*, **27**(9-12), pp. 563-571 (2018).
- 13) J. Uozumi: Generation and properties of laser speckle with long correlation tails, *Proc. SPIE 4705 (Saratov Fall Meeting 2001: Coherent Optics of Ordered and Random Media II)* pp. 95-106 (2002).
- 14) J. Uozumi: Fractality of the optical fields scattered by power-law-illuminated diffusers, *Proc. SPIE 4602 (Fifth International Conference on Correlation Optics)*, pp. 257-267 (2002).
- 15) J. Uozumi: Random optical fields with long spatial correlation, *Technical Digest of Fourth Japan-Finland Joint Symposium on Optics in Engineering (OIE'01)*, Osaka, Japan, pp. 13-14 (2001).
- 16) M. V. Berry: Diffractals, *J. Phys. A: Math. Gen.*, **12**, pp. 781-797 (1979).
- 17) J. Feder: *Fractals*, Plenum, New York, 1988.
- 18) H. Takayasu: *Fractals in the Physical Science*, Manchester University, Manchester, 1990.
- 19) T. Vicsek: *Fractal Growth Phenomena (Second Edition)*, World Scientific, Singapore, 1992.
- 20) S. K. Sinha: Scattering from fractal structures, *Physica D*, **38**, pp. 310-314 (1989).
- 21) J. Uozumi and T. Asakura: Optical Fractals, in *Optical Storage and Retrieval - Memory, Neural Networks, and Fractals*, ed. F. T. Yu and S. Jutamulia, chap.9, Macel Dekker, New York, 1996.
- 22) J. W. Goodman: Statistical properties of laser speckle pattern, in *Laser Speckle and Related Phenomena*, ed. J. C. Dainty (Second Enlarged Edition), pp. 9-75, Springer,

- Berlin, 1984.
- 23) J. W. Goodman: *Speckle Phenomena in Optics, Theory and Applications*, Roberts, Englewood, 2007.
- 24) J. Uozumi and T. Nakazawa: Generation of Anisotropic Fractal Speckle (in Japanese), *Bull. Faculty Eng., Hokkai-Gakuen Univ.*, No. 49, pp. 63-76 (2022).